DOI: 10.1002/ejoc.200901396

Complete Lipooligosaccharide Structure of the Clinical Isolate *Acinetobacter baumannii*, Strain SMAL

Eleonora Fregolino,[a] Giulia Fugazza,[b] Eugenio Galano,[a] Valentina Gargiulo,[a] Paolo Landini,[c] Rosa Lanzetta,[a] Buko Lindner,[d] Laura Pagani,[b] Michelangelo Parrilli,[a] Otto Holst,*[e] and Cristina De Castro*[a]

Keywords: Structure elucidation / Mass spectrometry / Glycolipids / NMR spectroscopy

Acinetobacter baumannii is a pathogenic organism that posesses a serious health threat because of the occurrence of the large number of (multi)drug-resistant strains. It can persist for prolonged periods in the hospital environment, infecting debilitated or immune-compromised patients. In this context, the endotoxin portion of the lipopolysaccharide, the lipid A, plays an important role in the pathogenesis of this bacterium, because it triggers the innate immune response and contributes to the inflammation state of the patient. In this study, the complete structure of the lipooligosaccharide has been determined. The saccharide backbone of the molecule was disclosed through chemical and spectroscopic analysis, whereas the lipid A moiety required detailed MS spectrometry and chemical investigations. The oligosaccharide backbone was found to be similar to that of *A. baumannii* ATCC 19606, although the LOS from the SMAL strain presented an enhanced zwitterionic character. The lipid A moiety comprises a heterogeneous and complex mixture of molecules: it possesses a conserved diphosphorylated disaccharide backbone substituted by three to seven fatty acids. The hexaacylated species appeared as the most abundant, and its chemical features, namely the number and the types of fatty acids, indicates its potential endotoxic activity.

Introduction

Acinetobacter baumannii is a Gram-negative bacterium and is considered an important emerging pathogen in hospital-acquired infections. Its clinical significance is related to its low susceptibility to most antibiotics commonly used such that many strains are now classified as pan-drug resistant.[1]

The growing incidence of nosocomial infections has promoted a significant increase in *Acinetobacter*-related studies. The most common pathogens belong to the so-called *A. calcoaceticus–A. baumannii* complex,[2] and the diseases commonly associated with these bacterial species are urinary tract infections, meningitis and sepsis. The disease outcome depends on the site of infection and on the patient's susceptibility.

The mechanism by which *Acinetobacter* is able to express its pathogenicity has not yet been completely elucidated, but a crucial role is played by components of the cell envelope outer membrane, namely the lipopolysaccharide (LPS) and capsular polysaccharides (CPS). These molecules act in synergy by blocking the access of human complement factors to the bacterial cell wall, which prevents bacterial killing and lysis.[3]

In this context, the establishment of the CPS and LPS structures is of importance for understanding the physical assemblage of the outer membrane and its properties, for example, adhesion to surfaces (i.e., hospital furniture or human skin), permeability to hazardous compounds (e.g., detergents used to clean surfaces) and the endotoxic power resident in the lipid A (LA) moiety of the LPS or lipooligosaccharide (LOS), which is able to activate the innate immune system[4] and may result in septic shock with an often fatal outcome of such bacterial infection.

Lipid A represents the endotoxic centre of the LPS or LOS; however, its endotoxicity is strongly dependent on its structure. It comprises a family of molecules that possess an amino sugar disaccharide as the backbone, which in most cases is β-D-GlcpN-(1→6)-α-D-GlcpN. The first glu-

[a] Department of Organic Chemistry and Biochemistry, University of Napoli Federico II – Complesso Universitario Monte Sant'Angelo,
Via Cinthia 4, 80126 Napoli, Italy
Fax: +39-081-674124
E-mail: decastro@unina.it
[b] Dipartimento di Scienze Morfologiche, Eidologiche e Cliniche, Università di Pavia,
Via Brambilla 74, 27100 Pavia, Italy
[c] Dipartimento di Scienze Biomolecolari e Biotecnologiche, Università di Milano,
Via Caloria 26, 20133 Milano, Italy
[d] Division of Immunochemistry, Research Center Borstel, Leibniz Center for Medicine and Biosciences,
23845 Borstel, Germany
[e] Division of Structural Biochemistry, Research Center Borstel, Leibniz Center for Medicine and Biosciences,
23845 Borstel, Germany
Fax: +49-4537-188-745
E-mail: oholst@fz-borstel.de

Supporting information for this article is available on the WWW under http://dx.doi.org/10.1002/ejoc.200901396.

cosamine is named GlcN-II or the non-reducing unit of the backbone, and the second is the GlcN-I or the reducing moiety. This oligosaccharide is substituted with fatty acids (mostly between 10 and 18 carbon atoms) and further decorated with two phosphate groups, one at O-1 of GlcN-I and the second at O-4 of GlcN-II. Usually, the heterogeneity of the LA is largely due to the fatty acid substituents, the number and length of which may vary, giving rise to penta-, hexa- or heptaacylated species. All these species are present in many LA preparations; however, their relative proportions are characteristic of specific bacterial species and are modulated by environmental stimuli.

The endotoxicity of differently acylated LA molecules depends on the presence of phosphate groups and the number and size of the fatty acids. Thus, a diphosphorylated and hexaacylated species, as is present in, for example, *Escherichia coli* LPS, acts highly agonistically, whereas less acylated species are less efficient or act even as antagonists.[5]

In this work, the complete structure of the lipooligosaccharide from the *A. baumannii* strain SMAL was investigated to gain valuable information that will provide an understanding of the mechanisms of activity adopted by this successful emerging pathogen.

Results and Discussion

LOS Chemical Analysis

Freeze-dried bacterial cells were extracted with phenol/chloroform/light petroleum (PCP).[6] The LOS was found to be composed of D-glucose (Glc), 2-amino-2-deoxy-D-glucosamine (GlcN), 2-amino-2-deoxy-D-galactosamine (GalN), 3-deoxy-*manno*-oct-2-ulosonic acid (Kdo) and 2-amino-2-deoxy-glucuronic acid (GlcNA).

The fatty acids were analysed by GC/MS as the methyl ester derivatives. The combined information concerning the total and *O*-linked composition identified the following ester-linked fatty acids: dodecanoic (12:0), 2-hydroxydodecanoic [12:0(2-OH)] and 3-hydroxydodecanoic [12:0(3-OH)] acid. 3-Hydroxytetradecanoic acid [14:0(3-OH)] is amide-linked. The 3-hydroxy fatty acids are (*R*)-configured and the 2-hydroxy fatty acids are (*S*)-configured.[7]

NMR Analysis of Core Oligosaccharides 2 and 3

The primary structure of the entire core oligosaccharide **1** (Figure 1) was deduced by combining the NMR spectroscopic data of the products isolated by alkaline degradation and acid hydrolysis. The first approach provided the structure of the incomplete core oligosaccharide **2** (Figure 1). Information regarding the unit(s) lost during the alkaline treatment was recovered by analysing the product **3** (Figure 1) obtained by mild acid hydrolysis.

The product isolated after strong alkaline degradation provided the truncated core oligosaccharide (**2**, Figure 1) comprising the lipid A sugar backbone and a 2-amino-2-deoxyuronic acid derivative possessing a double bond conjugated to the carboxy group (ΔHexNA), which results from β-elimination of the 4-substituted GlcNA.

The ^{1}H NMR spectrum of **2** (Figure 2a) contains eight anomeric signals and three sets of diastereotopic methylene signals due to the presence of three Kdo residues. A detailed analysis of both the homo- and heteronuclear NMR spectra (see Table 1 in the Supporting Information) of **2** led to the complete assignment of its proton and carbon chemical shifts, which revealed its structure (**2**, in Figure 1). Because the substituent at O-4 of ΔHexNA was lost during the alkaline treatment of the LPS, the product obtained from mild acid hydrolysis (**3**, Figure 1) was analysed by

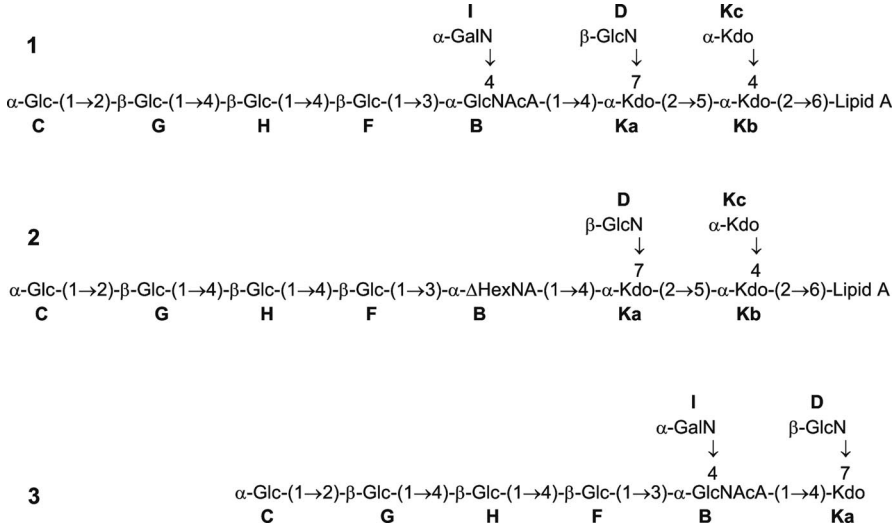

Figure 1. **1**: Complete structure of the oligosaccharide backbone of the LOS from *Acinetobacter baumannii* SMAL. All sugars are D-configured. **2**: Product isolated after complete LOS delipidation. ΔHexNA is a hex-4-en-2-aminuronic residue that results from β-elimination, the two glucosamines of the lipid A backbone are labelled **E** (non-reducing or GlcN-II) and **A** (reducing unit or GlcN-I). **3**: Oligosaccharide structure obtained from LOS after mild acid hydrolysis. The complete lipid A structure is reported in Figure 4.

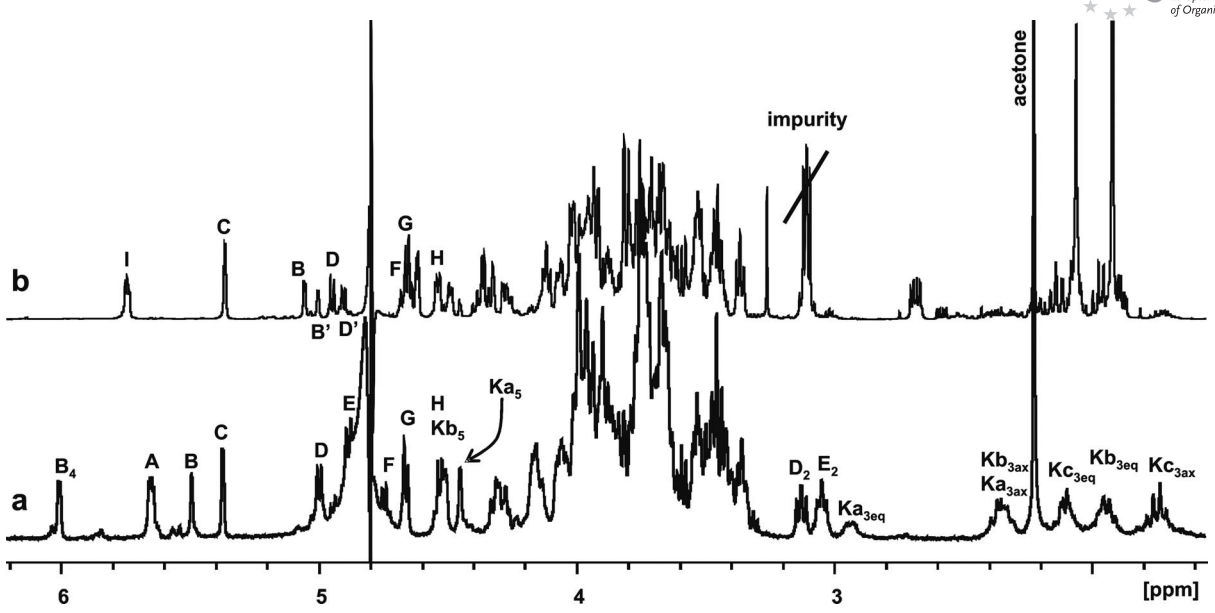

Figure 2. (a) ^{1}H NMR spectrum (500 MHz, 296 K, D_2O) of oligosaccharide **2** derived from the total delipidation of *A. baumannii* LOS. (b) ^{1}H NMR spectrum (600 MHz, 300 K, D_2O) of oligosaccharide **3** derived from LOS after mild acid hydrolysis. Residues **A** and **E** are the nonreducing and reducing glucosamines of lipid A, respectively. The residues close to the free reducing end of the oligosaccharide give rise to different signals in the spectrum, like **B** and **B′**, because their magnetic environment is affected by the different ring forms of the reducing Kdo residue. In both spectra, signals are labelled in accord with Figure 1.

NMR spectroscopy, which revealed an additional monosaccharide residue, unit **I** (Figure 2b, NMR spectroscopic data in Table 2 of the Supporting Information), but lacked the lipid A moiety (residues **A** and **E**) and the two Kdo units (**Kb** and **Kc**) as expected.

Combining the information from both **2** and **3**, the complete structure of the core oligosaccharide was determined as oligosaccharide **1** (Figure 1). Surprisingly, this structure is equivalent to that previously described for *A. baumannii* strain ATCC 19606.[8]

Electrospray Ionization Fourier-Transform Ion Cyclotron Resonance Mass Spectrometry (ESI-FT-ICR MS) Analysis of Intact and Ammonia-Deacylated Lipid A

The charge-deconvoluted mass spectrum obtained in the negative ion mode of the intact LA (Figure 3) comprises five groups of molecular peaks that originate from the intrinsic heterogeneity caused by the type and number of fatty acids linked to the disaccharide backbone. Each set of signals is labelled with a letter and, within each set, the different peaks are distinguished by numbers. Accordingly, group **a** is composed of a heptaacylated species, **b** of a hexaacylated, **c** of a pentaacylated, **d** of a tetraacylated and **e** of a triacylated species (Table 1).

In particular, the composition of the predominant species $\mathbf{b_1}$ (Table 1, Figure 4) is consistent with the occurrence of two 14:0(3-OH), two 12:0(3-OH), one 12:0(2-OH), one 12:0 and two phosphate units, $\mathbf{b_2}$ is related to $\mathbf{b_1}$ but 12:0(2-OH) is replaced by 12:0, $\mathbf{b_3}$ differs from $\mathbf{b_1}$ by the replacement of 14:0(3-OH) with 12:0(3-OH), and $\mathbf{b_4}$ from $\mathbf{b_3}$ by the replacement of 12:0(2-OH) with 12:0.

The presence of one 12:0(2-OH), as identified in the chemical analysis, was confirmed by the difference of 16 u between different couples of molecular peaks, for example, $\mathbf{b_1} - \mathbf{b_2}$ or $\mathbf{b_3} - \mathbf{b_4}$. This difference indicates the replacement of the 12:0(2-OH) unit by one 12:0, a substitution that is only possible for secondary and not primary fatty acids, which are always hydroxylated at C-3.

The species $\mathbf{b_5}$ to $\mathbf{b_7}$ have the same lipid composition as shown for $\mathbf{b_1}$, $\mathbf{b_2}$, $\mathbf{b_4}$, respectively, except that one phosphate group is missing.

A similar pattern was identified for almost all the other peak clusters, although some peaks were missing, probably due to their low abundance. Considering $\mathbf{b_1}$ as a reference, the homologous species in the other clusters were identified as follows (Figure 4): $\mathbf{a_1}$ contains one additional 12:0, $\mathbf{c_1}$ is missing one 12:0(3-OH), $\mathbf{d_1}$ lacks one 12:0(3-OH) and one 12:0, and $\mathbf{e_1}$ has two 14:0(3-OH) and one 12:0(2-OH) fatty acid residues. The occurrence of 12:0(2-OH) in every cluster is indicated by the presence of peaks differing by 16 u, as discussed above. Therefore, considering the composition of $\mathbf{b_1}$, the location of the four primary fatty acids was straightforward: the two amide-linked 14:0(3-OH) units are amide-linked, whereas the other two 3-hydroxy-bearing fatty acids are ester-bound substituents at O-3 of each glucosamine residue (Figure 4). The location of the two secondary fatty acids was inferred by analysis of the infrared multiphoton dissociation MS/MS data recorded in the positive ion mode or the molecular ions complexed with triethylamine.[9]

Under such conditions, $[\mathbf{b_1} + TEA]^+$ at m/z = 1830.4 u produced an abundant oxonium fragment ion at m/z = 1046.8 u (structure shown in Figure 4), representative of the nonreducing glucosamine moiety of LA with its substitu-

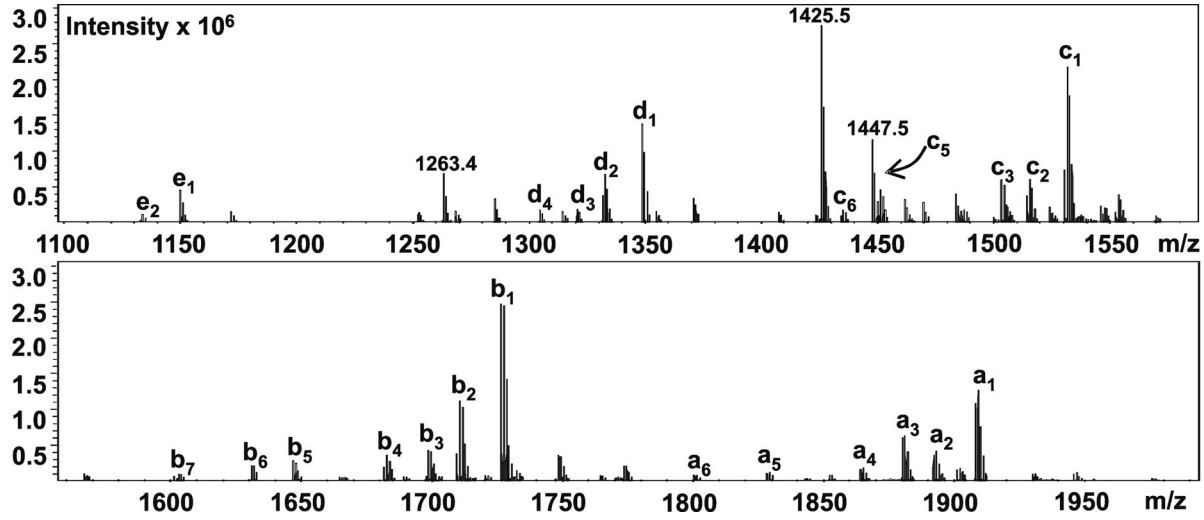

Figure 3. Pseudomolecular peaks of the *Acinetobacter baumannii* strain SMAL lipid A family measured by negative ion ESI-FT-ICR MS (structures are presented in Figure 4). The peaks at *m/z* = 1447.5, 1425.5 and 1263.4 and other minor peaks are impurities not related to lipid A.

Table 1. Lipid A species identified by ESI-FT-ICR MS (spectrum in Figure 3, structures in Figure 4) in *Acinetobacter baumannii* strain SMAL. The two glucosmine units have been omitted.

Mass [Da]	Rel. int. [%]	Species	No. of acyl groups	Proposed composition
1911.3	51.8	$\mathbf{a_1}$	7	2×14:0(3-OH), 2×12:0(3-OH), 12:0(2-OH), 2×12:0, 2×P
1895.3	17.0	$\mathbf{a_2}$	7	2×14:0(3-OH), 2×12:0(3-OH), 3×12:0, 2×P
1883.3	28.0	$\mathbf{a_3}$	7	14:0(3-OH), 3×12:0(3-OH), 12:0(2-OH), 2×12:0, 2×P
1867.3	8.0	$\mathbf{a_4}$	7	14:0(3-OH), 3×12:0(3-OH), 3×12:0, 2×P
1831.3	4.8	$\mathbf{a_5}$	7	2×14:0(3-OH), 2×12:0(3-OH), 12:0(2-OH), 2×12:0, P
1803.3	3.2	$\mathbf{a_6}$	7	14:0(3-OH), 3×12:0(3-OH), 12:0(2-OH), 2×12:0, P
1729.1	100	$\mathbf{b_1}$	6	2×14:0(3-OH), 2×12:0(3-OH), 12:0(2-OH), 12:0, 2×P
1713.1	46.2	$\mathbf{b_2}$	6	2×14:0(3-OH), 2×12:0(3-OH), 2×12:0, 2×P
1700.1	17.5	$\mathbf{b_3}$	6	14:0(3-OH), 3×12:0(3-OH), 12:0(2-OH), 12:0, 2×P
1685.1	14.3	$\mathbf{b_4}$	6	14:0(3-OH), 3×12:0(3-OH), 2×12:0, 2×P
1649.2	11.4	$\mathbf{b_5}$	6	2×14:0(3-OH), 2×12:0(3-OH), 12:0(2-OH), 12:0, P
1633.2	8.5	$\mathbf{b_6}$	6	2×14:0(3-OH), 2×12:0(3-OH), 2×12:0, P
1605.1	3.6	$\mathbf{b_7}$	6	14:0(3-OH), 3×12:0(3-OH), 2×12:0, P
1531.0	86.9	$\mathbf{c_1}$	5	2×14:0(3-OH), 12:0(3-OH), 12:0(2-OH), 12:0, 2×P
1515.0	24.6	$\mathbf{c_2}$	5	2×14:0(3-OH), 12:0(3-OH), 2×12:0, 2×P
1502.9	24.1	$\mathbf{c_3}$	5	14:0(3-OH), 2×12:0(3-OH), 12:0(2-OH), 1×12:0, 2×P
1485.9	7.2	$\mathbf{c_4}$	5	14:0(3-OH), 2×12:0(3-OH), 2×12:0, 2×P
1451.0	18.3	$\mathbf{c_5}$	5	2×14:0(3-OH), 12:0(3-OH), 1×12:0(2-OH), 12:0, P
1435.0	7.0	$\mathbf{c_6}$	5	2×14:0(3-OH), 12:0(3-OH), 2×12:0, P
1347.8	55.8	$\mathbf{d_1}$	4	2×14:0(3-OH), 12:0(3-OH), 12:0(2-OH), 2×P
1332.8	15.5	$\mathbf{d_2}$	4	2×14:0(3-OH), 12:0(3-OH), 12:0, 2×P
1320.8	7.5	$\mathbf{d_3}$	4	14:0(3-OH), 2×12:0(3-OH), 12:0(2-OH), 2×P
1304.8	7.0	$\mathbf{d_4}$	4	14:0(3-OH), 2×12:0(3-OH), 12:0, 2×P
1150.6	18.0	$\mathbf{e_1}$	3	2×14:0(3-OH), 12:0(2-OH), 2×P
1134.6	1.2	$\mathbf{e_2}$	3	2×14:0(3-OH), 12:0, 2×P

ents, one phosphate, one 14:0(3-OH), one 12:0(2-OH), one 12:0(3-OH) and one 12:0. On the basis of this information, the two secondary fatty acids identified in $\mathbf{b_1}$ were located on the nonreducing glucosamine moiety. The same oxonium ion was observed for the $\mathbf{a_1}$ and $\mathbf{c_1}$ species. The exact positions of the ester-linked fatty acids was inferred by analysis of the ammonia-treated LA: this chemical treatment preferentially removes the ester-linked acyloxyacyl esters leaving the amide-linked ones and their acyloxy substituents.[10] Accordingly, analysis of the charge-deconvoluted ESI spectrum (Figure 5) of the ammonia-treated LA allowed the identification of the secondary fatty acids on the corresponding primary residues: it contains three different clusters, named **f**, **g** and **h**, which are consistent with tetra-, tri- and diacylated species, respectively (Table 2). The more informative clusters were **f** and **g**, whereas the diacylated species $\mathbf{h_1}$ to $\mathbf{h_3}$ were identified as side-products of the ammonia-induced removal of the secondary fatty acid located on the amide-linked acyl residue of both the **f** and **g** clusters.

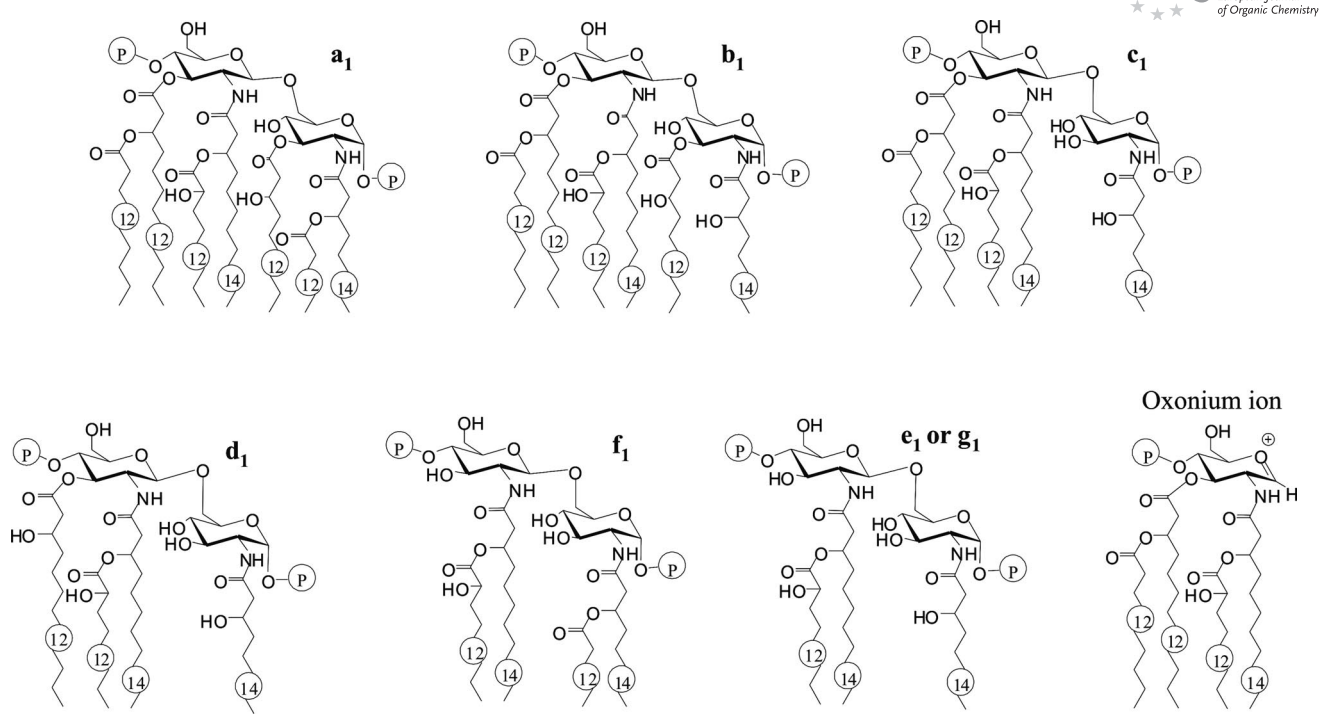

Figure 4. Structures of the lipid A molecules from *Acinetobacter baumannii* strain SMAL. Species from $\mathbf{a_1}$ to $\mathbf{e_1}$ were detected in the intact lipid A and molecules $\mathbf{f_1}$ and $\mathbf{g_1}$ were obtained from ammonia-treated lipid A. $\mathbf{a_1}$, $\mathbf{b_1}$ and $\mathbf{c_1}$ yielded the same oxonium ion.

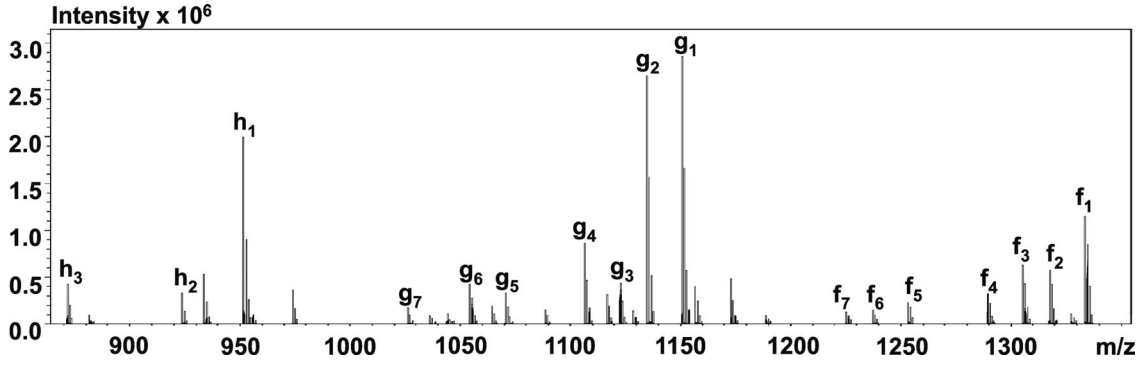

Figure 5. Pseudomolecular peaks identified in negative ion ESI-FT MS (structures shown in Figure 4) of ammonia-treated lipid A from *Acinetobacter baumannii* strain SMAL.

The predominant species, $\mathbf{g_1}$ (Figure 5, Table 2), is composed of two 14:0(3-OH), one 12:0(2-OH) and two phosphates. The distribution pattern within each cluster is similar to that of the intact LA, that is, the substitution of 12:0(2-OH) by 12:0, the replacement of one 14:0(3-OH) by one 12:0(3-OH) and the absence of one phosphate unit.

The information from the ion $\mathbf{g_1}$ was combined with the information provided by the oxonium ion (structure shown in Figure 4) deriving from $\mathbf{b_1}$ of the intact LA. According to the composition of the oxonium ion, hexaacylated species $\mathbf{b_1}$ possesses two secondary fatty acids on the nonreducing glucosamine, one 12:0(2-OH) and one 12:0. The finding that only 12:0(2-OH) was left after ammonia treatment indicates that this fatty acid is linked to the amide-linked 14:0(3-OH), whereas the other, 12:0, which was removed during the chemical treatment, is linked to 12:0(3-OH). Thus, the locations of the secondary fatty acids composing the penta-, tetra- and triacylated species in the intact LA were determined (Figure 4).

The mass distribution in cluster **f** indicates the occurrence of another tetraacylated LA with a fatty acid composition different to that described for the tetraacylated LA in the intact sample (cluster **d**), which reflects the distribution of the ester-bound acyl chains on the primary amide-linked fatty acids of the original heptaacylated LA family (cluster **a**).

From the above information the structure of the heptaacylated species was assigned. Cluster $\mathbf{f_1}$ is composed of two 14:0(3-OH), one 12:0(2-OH), one 12:0 and two phosphates. Therefore, $\mathbf{f_1}$ contains one additional 12:0 compared with $\mathbf{g_1}$: the only position available on the disaccharide backbone for 12:0 is at 14:0(3-OH) on GlcN-I, thus yielding the structures of both $\mathbf{f_1}$ and $\mathbf{a_1}$ as depicted in Figure 4.

Table 2. Molecular species of ammonia-treated lipid A from *Acinetobacter baumannii* strain SMAL identified by ESI-FT-ICR MS (spectrum shown in Figure 5, structures in Figure 4). The two glucosamine units have been omitted.

Mass [Da]	Rel. int. [%]	Species	No. of acyl groups	Proposed composition
1332.8	40.9	$\mathbf{f_1}$	4	2×14:0(3-OH), 12:0(2-OH), 12:0, 2×P
1316.8	20.1	$\mathbf{f_2}$	4	2×14:0(3-OH), 2×12:0, 2×P
1304.8	22.0	$\mathbf{f_3}$	4	14:0(3-OH), 12:0(3-OH), 12:0(2-OH), 12:0, 2×P
1288.8	11.6	$\mathbf{f_4}$	4	14:0(3-OH), 12:0(3-OH), 2×12:0, 2×P
1252.8	11.6	$\mathbf{f_5}$	4	2×14:0(3-OH), 12:0(2-OH), 12:0, P
1236.8	5.1	$\mathbf{f_6}$	4	2×14:0(3-OH), 2×12:0, P
1224.8	4.6	$\mathbf{f_7}$	4	14:0(3-OH), 12:0(3-OH), 12:0(2-OH), 12:0, P
1150.6	100	$\mathbf{g_1}$	3	2×14:0(3-OH), 12:0(2-OH), 2×P
1134.6	95.8	$\mathbf{g_2}$	3	2×14:0(3-OH), 12:0, 2×P
1122.6	15.6	$\mathbf{g_3}$	3	14:0(3-OH), 12:0(3-OH), 12:0(2-OH), 2×P
1106.6	30.1	$\mathbf{g_4}$	3	14:0(3-OH), 12:0(3-OH), 12:0, 2×P
1070.6	11.6	$\mathbf{g_5}$	3	2×14:0(3-OH), 12:0(2-OH), P
1054.7	14.8	$\mathbf{g_6}$	3	2×14:0(3-OH), 12:0, P
1026.6	6.2	$\mathbf{g_7}$	3	14:0(3-OH), 12:0(3-OH), 12:0, P
952.5	69.8	$\mathbf{h_1}$	2	2×14:0(3-OH), 2×P
934.5	18.5	$\mathbf{h_2}$	2	14:0(3-OH), 12:0(3-OH), 2×P
872.5	14.9	$\mathbf{h_3}$	2	2×14:0(3-OH), P

Conclusions

In this report the complete structure of the LOS of *Acinetobacter baumannii* strain SMAL is reported. The sequence of the core oligosaccharide was achieved through the combined use of chemical and spectroscopic procedures. The backbone is formed of 12 sugar residues, which are organized as a highly branched inner core moiety and is equivalent to one of the structures reported for *A. baumannii* ATCC 19606.[8] This region contains a motif that could be present within the *A. baumannii* LPS;[8,11] however, it is also present in the core region of LPS from *A. radioresistens*.[12]

In contrast to the core region of LPS from *A. baumannii* ATCC 19606, the galactosamine linked to GlcNAcA is not *N*-acetylated, and the core oligosaccharide is not truncated. These features might reflect the adaptation of the bacterium to the host environment, in particular, the cationic amino sugars decrease the net negative charge of the core region and thus might shield the bacterial membrane from the effect of host defence agents, like the cationic antimicrobial peptides.

Regarding the endotoxic moiety of the LOS, high-resolution ESI-FT MS revealed that lipid A is formed of a heterogeneous blend of molecules, which contain the conserved diphosphorylated glucosamine disaccharide backbone variously substituted with fatty acid residues, ranging from tri- through to heptaacylated molecules (Figure 4 and Table 1).

Each cluster comprises different species due to the non-stoichiometric replacement of (*S*)-12:0(2-OH) with 12:0, (*R*)-14:0(3-OH) with (*R*)-12:0(3-OH) or from the lack of one phosphate unit. Within *Acinetobacter*, (*S*)-12:0(2-OH) has so far only been reported for the LPS of *A. radioresistant*,[13] in which it is present in only small amounts. The finding of this fatty acid supports the putative function of two genes from *A. baumannii*, deposited in the PubMed database,[14] for which fatty acid 2-*O*-hydroxylase activity was predicted on the basis of sequence homology with other enzymes.

With regard to the fatty acid pattern, the prominent lipid A species is the hexaacylated one, similar to the agonistic endotoxin present in the LPS of *E. coli*, comprising six fatty acids with a chain length of 14 and/or 12 carbon atoms distributed asymmetrically on the glucosamine disaccharide backbone.[15]

Experimental Section

Bacterial Identification and Genotyping: The *Acinetobacter baumannii* SMAL strain was a multidrug-resistant (MDR) clinical isolate representative of a clonal lineage causing nosocomial infections, including sepsis, in different Italian settings and recovered since 2002. The isolate was identified by using the Vitek 2® automated instrument ID system (BioMérieux, Marcy l'Etoile, France) and sequencing of the blaOXA-51-like gene.[16] Species identification was also confirmed by using the *gyrB* PCR method previously described.[17] Genomic relatedness among *A. baumannii* isolates was investigated by pulsed-field gel electrophoresis (PFGE).[18]

Cell Growth and Isolation of LPS: The *Acinetobacter baumannii* strain SMAL was grown in a liquid shake culture in LB medium at 28 °C (20 L). Cells in the early stationary phase, were collected by centrifugation (9800 g, 20 min, 4 °C), washed sequentially with distilled water, ethanol, acetone and diethyl ether and finally freeze-dried. The LOS was isolated on dry cells (yield 0.3 g/L) by aqueous 90% phenol/chloroform/light petroleum (2:8:5, v/v/v) extraction.[6] After removal of the light solvents under vacuum, LOS was precipitated from phenol with water and washed with aqueous 80% phenol and acetone. The pellet was then suspended in water and lyophilized (43 mg, yield 7.2 mg/g_{cells}).

General and Analytical Procedures: The total fatty acid content and monosaccharide composition were determined by treating LPS with methanolic HCl at 80 °C for 18 h. The solution was extracted twice with equal volumes of *n*-hexane, the two top layers (*n*-hexane)

were combined and dried, and the fatty acid methyl esters were analysed directly by GC/MS. The bottom layer (methanol) was dried with a stream of air, and the resulting methyl glycosides were acetylated, as reported elsewhere.[19] The absolute configuration was determined by analysis of the chiral 2-octyl[20] or 2-butyl[21] derivatives. The ester-bound fatty acids were selectively released from LPS by base-catalysed hydrolysis (0.5 M NaOH, 37 °C, 2 h); the solution was acidified to pH = 4.0 by dropwise addition of 1 M HCl and extracted twice with an equal volume of $CHCl_3$. Fatty acids were recovered from the organic layer, esterified with diazomethane and analysed by GC/MS. Each methyl ester derivative was identified by comparison of its retention time with that of the reference compound and by its MS fragmentation. All GC/MS analyses were performed with a Hewlett–Packard 5890 instrument equipped with an SPB-5 capillary column (Supelco, 30 m × 0.25 i.d., flow rate 0.8 mL/min, He as carrier gas) with the following temperature program: 150 °C for 3 min, 150 → 300 °C at 10 °C/min, 300 °C for 18 min. EI MS data were recorded with an ionization energy of 70 eV and an ionizing current of 0.2 mA.

Isolation of Core Oligosaccharides 2 and 3 and Preparation of Intact and Ammonia-Deacylated Lipid A: Total delipidation procedure of the LOS was carried out as reported previously;[22] namely, the sample (20 mg) was deesterified by hydrazinolysis, deamidated by strong alkaline hydrolysis and desalted by size-exclusion chromatography on a Sephadex G10 column. Finally, the oligosaccharide was further purified by HPLC on a TSK-3000 PW_{XL} size exclusion column eluting with water at a flow rate of 0.8 mL/h (product **2**, 3 mg, structure shown in Figure 1). Another LPS portion (15 mg) was hydrolysed in aq. 1% AcOH (100 °C, 2 h), the precipitate (lipid A, 5 mg) was removed by centrifugation, and the supernatant was lyophilized and fractionated by GPC on a TSK HW-40 column. Oligosaccharide **3** (8 mg, Figure 1) was the first compound eluted and was used directly in spectroscopic studies. The selective ester-bound acyloxyacyl deacylation promoted by ammonia treatment was performed directly on lipid A (200 μg) by 1% AcOH LOS hydrolysis as reported previously.[10]

Mass Spectrometry: ESI-FT-ICR MS was performed in negative and positive ion modes with a hybrid Apex Qe FT-ICR mass spectrometer (Bruker Daltonics, Billerica, MA, USA), equipped with a 7 T superconducting magnet and an Apollo dual ion source. The instrument was controlled by Bruker's ApexControl software, version 2.0.0.36, and data was recorded in broadband mode with 512K data sampling rate. The mass scale was calibrated externally by using compounds of known structure. For the negative ion mode samples (ca. 10 ng/μL) were dissolved in a 50:50:0.001 (v/v/v) mixture of 2-propanol/water/triethylamine (pH ≈ 8.5). For the positive ion mode samples, a 50:50:0.03 (v/v/v) mixture of 2-propanol/water/30 mM ammonium acetate adjusted with acetic acid to pH = 4.5 was used. The samples were sprayed at a flow rate of 2 μL/min. The capillary entrance voltage was set to 3.8 kV and the drying gas temperature to 150 °C. The spectra, which showed several charge states for each component, were charge-deconvoluted by using the DataAnalysis Software (Bruker Daltonics), and the mass numbers given refer to monoisotopic molecular masses. For unspecific fragmentation the voltage in the external collision cell was increased from 3 to 30 V. Infrared multiphoton dissociation (IRMPD) of isolated parent ions was performed with a 25 W, 10.6 μm CO_2 laser (Synrad, USA). The unfocused laser beam was directed through the centre of the trap. The duration of the laser irradiation was adapted to generate optimal fragmentation and varied between 10 and 80 ms. Fragment ions were detected after a delay of 0.5 ms.

NMR Spectroscopy: ^1H and ^1H-^{13}C NMR experiments on product **2** were carried out with a Varian Inova 500 spectrometer form Consortium INCA (L488/92, Cluster 11) equipped with a reverse probe operating at 296 K. The spectra of product **3** were recorded at 300 K with a Bruker DRX-600 spectrometer equipped with a cryogenic probe. All spectra were calibrated with respect to internal acetone (δ_H = 2.225 ppm; δ_C = 31.45 ppm). For all homonuclear spectra, experiments were measured with data sets of 2048 × 512 points, 32 scans were acquired, and mixing times of 200 and 120 ms were employed for ROESY and TOCSY experiments, respectively. Each data matrix was zero-filled in both dimensions to give a matrix of 4096 × 2048 points and was resolution-enhanced in both dimensions by a shifted sine-bell function before Fourier transformation. The HSQC experiment was performed by using a data set of 2048 × 512 points, whereas for the HMBC experiment a data set of 2048 × 256 points was used. For each t_1 value, 64 scans were acquired, and the HMBC sequence was optimized for a 6 Hz long-range coupling constant. All NMR spectra were acquired and transformed by using the Topspin 3.0a program and studied with Pronto software.[23]

Supporting Information (see footnote on the first page of this article): ^1H and ^{13}C NMR chemical shifts for oligosaccharides **2** and **3**.

Acknowledgments

The authors thank Regina Engel (Research Center Borstel) for technical assistance.

[1] A. Y. Peleg, H. Seifert, D. L. Paterson, *Clin. Microbiol. Rev.* **2008**, *21*, 538–582.
[2] M. L. Joly-Guillon, *Clin. Microbiol. Infect.* **2005**, *11*, 868–873.
[3] V. K. Goel, A. Kapil, *BCM Microbiol.* **2001**, *1*, 16–24.
[4] R. Medzhitov, *Nat. Rev. Immunol.* **2001**, *1*, 135–145.
[5] S. I. Miller, R. K. Ernst, M. W. Bader, *Nat. Rev. Immunol.* **2005**, *3*, 36–46.
[6] C. Galanos, O. Lüderitz, O. Westphal, *Eur. J. Biochem.* **1969**, *9*, 245–249.
[7] E. T. Rietschel, *Eur. J. Biochem.* **1976**, *64*, 423–428.
[8] E. V. Vinogradov, J. Ø. Duus, H. Brade, O. Holst, *Eur. J. Biochem.* **2002**, *269*, 422–430.
[9] A. Kondakova, A. B. Lindner, *Eur. J. Mass Spectrom.* **2005**, *11*, 535–546.
[10] A. Silipo, R. Lanzetta, A. Amoresano, M. Parrilli, A. Molinaro, *J. Lipid Res.* **2002**, *43*, 2188–2195.
[11] E. V. Vinogradov, B. O. Petersen, J. E. Thomas-Oates, J. Duus, H. Brade, O. Holst, *J. Biol. Chem.* **1998**, *273*, 28122–28131.
[12] S. Leone, A. Molinaro, P. Pessione, R. Mazzoli, C. Giunta, L. Sturiale, D. Garozzo, R. Lanzetta, M. Parrilli, *Carbohydr. Res.* **2006**, *341*, 582–590.
[13] S. Leone, L. Sturiale, P. Pessione, R. Mazzoli, C. Giunta, R. Lanzetta, D. Garozzo, A. Molinaro, M. Parrilli, *J. Lipid Res.* **2007**, *48*, 1045–1051.
[14] GeneIDs 5986103 and 6002532 at www.ncbi.nlm.nih.gov/pubMed.
[15] C. Alexander, E. T. Rietschel, *J. Endotox. Res.* **2001**, *7*, 167–202.
[16] J. F. Turton, N. Woodford, J. Glover, S. Yarde, M. E. Kaufmann, T. L. Pitt, *J. Clin. Microbiol.* **2006**, *44*, 2974–2976.
[17] P. G. Higgins, H. Wisplinghoff, O. Krut, H. Seifert, *Clin. Microbiol. Infect.* **2007**, *13*, 1199–1201.
[18] A. Endimiani, F. Luzzaro, R. Migliavacca, E. Mantengoli, A. M. Hujer, K. M. Hujer, L. Pagani, R. A. Bonomo, G. M. Rossolini, A. Toniolo, *Antimicrob. Agents Chemother.* **2007**, *51*, 2211–2214.

[19] O. Holst in *Methods in Molecular Biology, Bacterial Toxins: Methods and Protocols* (Ed.: O. Holst), Humana Press Inc., Totowa, NJ, **2000**, pp. 345–353.
[20] K. Leontein, J. Lönngren, *Methods Carbohydr. Chem.* **1978**, *62*, 359–362.
[21] G. J. Gerwig, J. P. Kamerling, J. F. G. Vliegenthart, *Carbohydr. Res.* **1978**, *62*, 349–357.
[22] V. Gargiulo, D. Garozzo, R. Lanzetta, A. Molinaro, L. Sturiale, C. De Castro, M. Parrilli, *ChemBioChem* **2008**, *9*, 1830–1835.
[23] M. Kjaer, K. V. Andersen, F. M. Poulsen, *Methods Enzymol.* **1994**, *239*, 288–308.

Received: December 1, 2009
Published Online: January 29, 2010

